JTTEE5 3:299-304


# On the Gas Dynamics of HVOF Thermal Sprays

*C.M. Hackett, G.S. Settles, and J.D. Miller*

**An experimental study of the gas-dynamic aspects of the high-velocity oxyfuel (HVOF) thermal spray process has been performed using commercially available HVOF equipment (Hobart-Tafa JP-5000, Hobart-Tafa Technologies, Inc., Concord, NH). Optical diagnostic techniques, including microsecond-exposure schlieren and shadowgraph imaging, were applied to visualize the hot supersonic jet produced by this equipment without particle injection. Rapid turbulent mixing of the jet with the surrounding atmosphere was observed, which is an issue of concern in coating quality due to the possibility of oxidation of sprayed particles. This mixing appears to be a function of the ratio of densities of the hot jet and the cold atmosphere as well as a function of the velocity of the jet, rather than one of combustion-chamber pressure or barrel length. The supersonic core of the HVOF jet dissipates rapidly due to the mixing, so that the jet is no longer supersonic when it impinges on the target surface being sprayed. Secondary issues also observed in this study include strong jet-noise radiation from the HVOF plume and the entrainment and induced bulk motion of the surrounding air.**

## 1. Introduction

THE high-velocity oxyfuel (HVOF) process is a recent development in the field of thermal spray coatings. The desirable properties of HVOF coatings, typically high density and low porosity, result from high spray-particle velocities produced by a hot, combustion-driven, high-speed gas jet. Although this process is centered in the field of advanced materials, the related field of gas dynamics governs the propagation of high-speed gas jets in the atmosphere and is thus intimately involved in HVOF technology.

To the authors' knowledge, there have been few studies of the gas dynamics of HVOF thermal sprays. Two groups of investigators (Ref 1, 2) have made measurements and performed analyses that relate to this issue. Computational fluid dynamics calculations that predict certain gas-dynamic aspects of the HVOF process have been carried out by another group (Ref 3, 4). Clearly, however, much more work is required to both understand and optimize HVOF gas dynamics.

Moreover, numerous issues of technology transfer are related to HVOF gas dynamics. Although the HVOF thermal spray process represents a new coating technology, in principle it amounts to a small gas- or liquid-fueled rocket motor. Rocket propulsion, of course, is a comparatively mature subfield of aerospace engineering (Ref 5). The key issue in rocket propulsion is high thrust with low weight, whereas neither the thrust nor the weight of an HVOF gun is a key issue compared to coating quality. Nonetheless, HVOF technology and rocket propulsion share many common points, not the least of which is the gas dynamics of a supersonic particle-laden jet issuing into the atmosphere.

Gas dynamics influences the HVOF spray process and the resulting coating in several ways. First, the particles injected into the gas stream must be accelerated by the jet in order to impact against the substrate at high velocity. It has been shown that several coating properties, primarily density and porosity, improve with increasing particle velocity (Ref 2). Second, heat transfer from the gas stream to the particles is required to raise spray-particle temperatures. Third, the economic advantage of thermal spraying in the open atmosphere carries with it the drawback that the atmosphere mixes rapidly with the spray jet. This can lead to oxidation of particles in flight and consequent deterioration of coating quality. Finally, several ancillary gas-dynamic issues arise, such as jet noise and secondary airflow due to entrainment. The spray process is inherently loud and presents a possible health hazard. Secondary airflow could lead to unwanted inclusions within a coating due to particulate matter circulating within the spray booth.

This investigation represents an initial effort to characterize the external gas dynamics of one example of an existing, commercially available HVOF spray gun. As such, it is limited to the flow visualization of the HVOF jet without particle injection. This discussion constitutes a broad overview of the principles of gas dynamics associated with HVOF sprays; quantitative analysis of specific issues has been left to subsequent investigations. Because all commercial HVOF equipment operates on similar principles, the results discussed herein are believed to apply in general to all such equipment, regardless of manufacturer.

**Key Words:** gas dynamics, jet flows, turbulent mixing, HVOF

**C.M. Hackett, G.S. Settles,** and **J.D. Miller,** Gas Dynamics Laboratory, Mechanical Engineering Department, Penn State University, University Park, PA, 16802, USA

## 2. Experimental Apparatus

### 2.1 *HVOF Thermal Spray Equipment*

The HVOF thermal spray system (Hobart-Tafa JP-5000, Hobart-Tafa Technologies, Inc., Concord, NH) used in this investigation consists of a control console, a spray gun, and a powder feeder (although no powder was sprayed during the present study). Cooling water for the gun is also required at the rate of 30 L/min (8 gal/min). High-pressure liquid fuel (kerosene) and gaseous oxygen feedlines supply the gun, where the fuel is atomized and mixed with the oxygen in the combustion chamber (Fig. 1). The combustion-chamber pressure, $P_C$, was set at values of 0.65, 0.78, or 0.91 MPa (95, 115, or 135 psia).

The hot gaseous products of combustion pass through a converging-diverging nozzle followed by a straight barrel. The flow at the nozzle exit/barrel entrance is estimated to be at about

Mach 2 based on area ratio calculations. Two barrel lengths, 10 and 20 cm (4 and 8 in.), are considered in these experiments. During normal operation of the thermal spray equipment, powder and carrier gas are fed into the hot gas stream at the entrance to the barrel. However, in the present tests only the carrier gas is supplied to the gun. The HVOF gun itself is rigidly mounted to a stand to properly position it relative to the flow-visualization apparatus.

### 2.2 *Schlieren Optics*

The schlieren technique is a key optical tool in the visualization and measurement of compressible flows (Ref 6). Its present implementation is rather unique because it provides a 1 m (40 in.) diam field of view with very high sensitivity through the use of a large, parabolic glass mirror. A discussion of the design and operation of this single-mirror, double-pass schlieren system is given by Settles (Ref 7). Images obtained by this technique are visualizations of the gradient of gas density within the optical field of view.

The flow-visualization data are collected principally by way of S-VHS videotaping of the real-time schlieren images; some color transparencies are also obtained. Selected frames from the videotape are digitized using a PC computer-based "frame grabber" and image processor and are presented as still images. When a tungsten-filament light source is used in the schlieren apparatus, frame exposures of $\frac{1}{60}$ s are obtained by the video camera. Alternatively, a xenon-arc light source is used to produce exposures in the microsecond range, effectively freezing the motion of the gas in the field of view. Shadowgraph visualizations (Ref 6) can be acquired using the same optical apparatus with the removal of the schlieren cutoff filter.

## 3. Results and Discussion

### 3.1 *Internal Gas Dynamics of the HVOF Gun*

Although the present study focuses on aspects of the gas flow once it has left the HVOF gun (external gas dynamics), it is useful to consider the processes internal to the gun that have a significant impact on the external flow. Because the internal gas dynamics of the Hobart-Tafa HVOF system used here has already been covered in detail by Thorpe and Richter (Ref 2), this discussion will be quite brief.

The atomized-fuel/oxygen mixture is burned in the combustion chamber to produce pressures up to 0.91 MPa (135 psia) and temperatures up to 3360 K (5590 °F). Due to cooling-water circulation the gas flow is certainly nonadiabatic. The products of combustion (hot gases), which have a specific-heat ratio of approximately 1.2, are accelerated to Mach 1 at the nozzle throat and then expanded to about Mach 2 at the juncture of the nozzle and the barrel.

The flow through the constant-area barrel of the HVOF gun is subject to the combined effects of friction and heat transfer. Such quasi-one-dimensional problems of combined frictional (Fanno) and heat-transfer (Rayleigh) flow are discussed in the classical gas dynamics literature (Ref 8). A solution of the fluid properties in the duct is possible with sufficient knowledge of the boundary conditions; however, that determination is beyond the scope of the present work. It is interesting to note, though, that friction tends to drive the flow at the barrel exit toward Mach 1, whereas heat transfer from the gas to the cooling water tends to do the opposite. In the present investigation, flow visualization reveals the gas leaving the HVOF barrel to be supersonic, with a static pressure of greater than 1 atm for all the present test conditions.

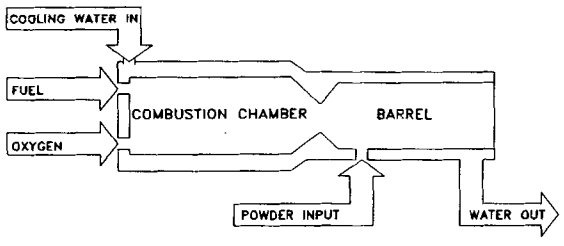


**Fig. 1** Schematic of the JP-5000 HVOF gun

### 3.2 *Shock Diamonds*

The flow leaving the HVOF barrel is known as an underexpanded axisymmetric supersonic freejet, because the static pressure of the jet in the immediate vicinity of the barrel exit is greater than ambient (atmospheric) pressure. The most noticeable feature of this jet flow is the presence of visible "shock diamonds" embedded within the initial mixing region of the developing jet (Ref 9). These diamond-shaped structures are naturally visible due to the light emitted by the hot gas. Their characteristic shape is the result of the repeated reflections of oblique pressure waves within the supersonic core of the jet as the gas flow expands and compresses in an attempt to reach an equilibrium with the surrounding atmosphere. Upon exiting the barrel, the flow first expands and its static temperature drops, and thus visible-light emission ceases. The jet tends to overshoot the ambient pressure condition, and a subsequent compression region raises the gas temperature and renders it visible once again. This pattern of expansion and recompression is repeated until the supersonic core of the jet is eventually dissipated by mixing with the surrounding atmosphere, as illustrated sche-

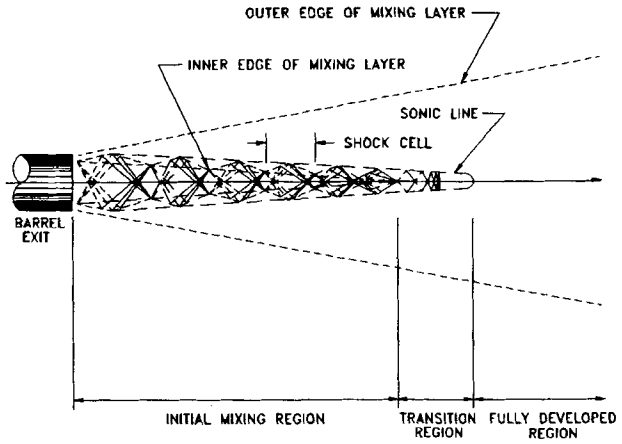


**Fig. 2** Diagram of an underexpanded supersonic jet plume

matically in Fig. 2. Similar shock-diamond phenomena may be seen on a much larger scale in the exhaust of rockets and turbojet engines. The geometric structure of the shock-diamond cells, such as the angles characterizing the shock waves, is determined by the Mach number at the exit of the barrel and the ratio of the jet exit-plane static pressure to atmospheric pressure. Furthermore, the length of the visible shock-diamond plume indicates the longitudinal extent of the supersonic core of the jet. However, the number of visible shock diamonds bears no simple relationship to the exit Mach number of the HVOF jet.

Figure 3(a) is an enlarged view of a single shock cell rendered visible due to its natural luminescence at the HVOF barrel exit. For comparison, Fig. 3(b) is a diagram of the similar flow pattern as predicted by a planar method of characteristics calculation. The method of characteristics is a mathematical technique for computing inviscid supersonic flows (Ref 8). This comparison is purely qualitative, but it does serve to illustrate the internal expansion and compression waves in the supersonic core of the jet that coalesce to form the shock diamonds.

Images of the supersonic jet core were recorded on videotape under their own natural luminescence. (In all of these visualizations, the actual exit of the barrel is obscured by the water-cooling jacket that surrounds it and that extends a short distance beyond it.) In Fig. 4, the visible core is shown for the long (20 cm, or 8 in.) barrel and for chamber pressures of 0.65 and 0.91 MPa (95 and 135 psia). In general, a higher chamber pressure results in a longer supersonic core. This is primarily due to an increase in static pressure at the barrel exit. The length of the barrel does not appear to have a strong influence on the supersonic core of the HVOF exhaust plume.

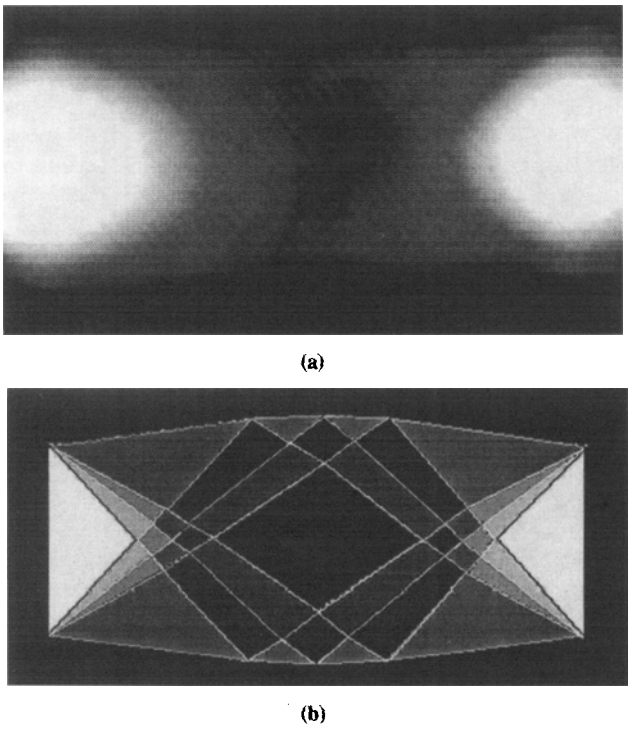

(a)

(b)

**Fig. 3** Shock cell of a HVOF jet. (a) Experiment under natural luminescence, $P_c = 0.91$ MPa (135 psia). (b) Planar characteristics calculation

The natural luminescence of the HVOF plume makes schlieren visualization of the shock diamonds difficult. As a comparative test, the jet is visualized while the gun is operated in a noncombusting mode, with the combustion chamber pressurized with cold gas (oxygen only). Shadowgraphy of the flow at the barrel exit reveals a highly unstable and irregular pattern of shock waves and turbulence that disintegrates only a short distance downstream. Figure 5 is such an image, highly magnified and frozen in time by microsecond strobe illumination.

### 3.3 *Turbulent Mixing*

As illustrated in Fig. 2, the mixing of the surrounding atmosphere with the hot HVOF exhaust jet limits the length of the supersonic core. Although this core is visible to the naked eye because of its high temperature, the mixing layer that surrounds it normally is not visible. To observe it, schlieren and shadowgraph images were taken of the HVOF exhaust plume.

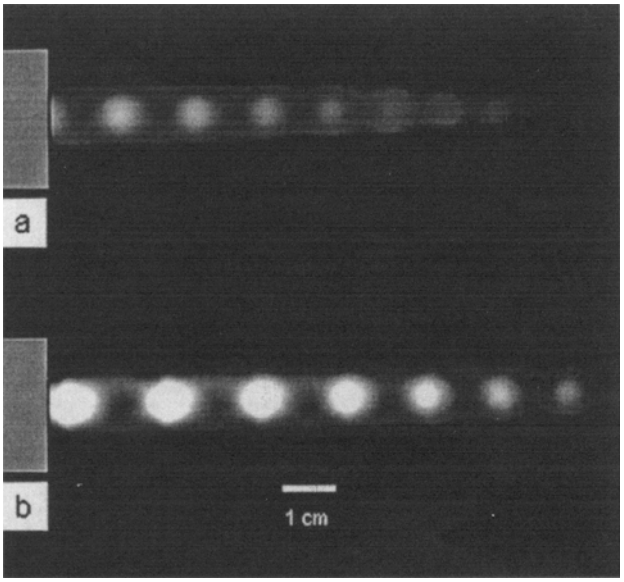


**Fig. 4** Images of shock diamonds. (a) $P_c = 0.65$ MPa (95 psia). (b) $P_c = 0.91$ MPa (135 psia)

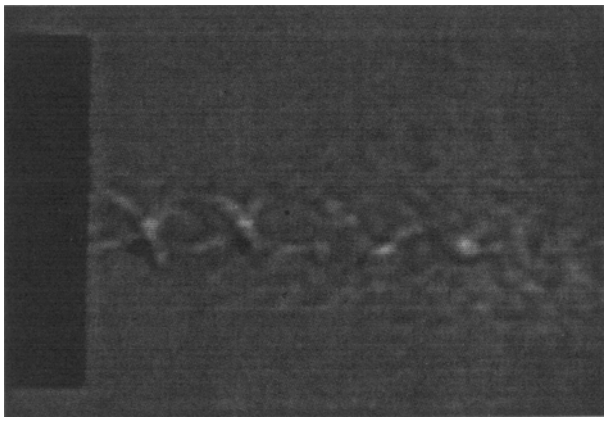

**Fig. 5** Microsecond shadowgram of disintegrated shock diamonds in cold jet

In the shadowgram shown in Fig. 6(a), the radiant supersonic core of the plume (the brightest region in the figure) is only a small part of the total flowfield, which also includes a large turbulent mixing zone that spreads in a conical manner from the exit of the barrel. Thus, a proper description of the HVOF flowfield must include not only the high-temperature visible core of the jet but also the substantial mixing region that surrounds it.

The outer diameter of the HVOF barrel-exit water jacket (see Fig. 6a) is 4.1 cm (1.6 in.). With this as a length reference, it may be noted that the right-hand boundary of Fig. 6(a) is within the recommended standoff distance of 30 to 40 cm (12 to 16 in.) between the barrel exit and the target being sprayed. The visible supersonic core region, however, is already dissipated after a distance of about 20 cm (8 in.) from the barrel exit. It is evident that the HVOF plume that actually impacts the target has already mixed sufficiently with the surrounding atmosphere to be entirely subsonic.

The mixing of the jet may affect the deposition of sprayed coatings in several ways. Turbulent mixing may reduce the velocity and temperature of the gas below the velocity and temperature of the spray particles, thus decelerating and cooling the particles well before impact with the target substrate. Measurements and computations of particle velocity (Ref 11) with similar HVOF equipment tend to confirm this notion. Efforts should be made to prevent particle deceleration prior to impact, because high particle velocities are important to the formation of dense coatings. Furthermore, although it is true that injected powder particles tend to remain near the centerline of the broadly expanding thermal plume shown in Fig. 6(a), the action of turbulent mixing is to entrain the surrounding atmosphere and transport it inward toward the centerline of the jet. Thus, oxygen is brought into proximity with the moving particles, creating the potential for oxidation to occur during flight. As oxide inclusions are generally considered to degrade coating performance, it may be assumed that turbulent mixing has the potential to adversely affect coating quality.

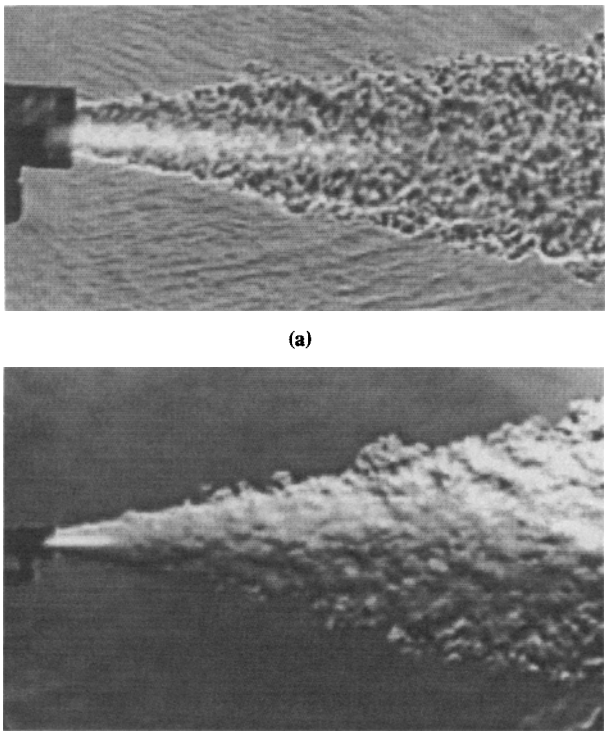

(a)

(b)

**Fig. 6** Visualization of HVOF mixing plume. (a) Closeup microsecond shadowgram. (b) Full-field schlieren image. Jet velocity ~2000 m/s (6560 ft/s); $\rho_{jet}/\rho_{atm} \sim 0.1$

Figure 6(b) is a schlieren image with the full 1 meter (40 in.) field of view of the optical instrument, showing the extent of the mixing region well downstream of the barrel exit. Also visible are some of the large-scale turbulent structures that are responsible for the entrainment of the surrounding atmosphere into the mixing region.

Although several factors may have an influence on the mixing rate, the two most significant appear to be the temperature of the jet (more specifically, the ratio of densities of the jet to the surrounding atmosphere, $\rho_{jet}/\rho_{atm}$) and the velocity of the jet. Noncombusting operation of the HVOF equipment with oxygen gas at ambient temperatures allowed examination of this issue through the visualization of a jet with a different density ratio and velocity exhausting from the same nozzle geometry. Schlieren images of the resulting flowfield were recorded over a range of chamber pressures from 0.65 to 1.50 MPa (95 to 220 psia), although little effect of the cold-gas chamber pressure is noted. However, a difference in the visual spreading rate of a typical cold jet (Fig. 7) when compared to the hot HVOF combustion jet (Fig. 6b) is clearly visible, the visible spreading rate of the hot jet being the greater of the two by a factor of 180%. This result is consistent with the classic study of density-ratio effects on the turbulent mixing of planar two-dimensional shear layers by Brown and Roshko (Ref 12). A decrease in the density of the primary (high-velocity) stream in their work was shown to increase the mixing rate. Increasing the ratio of primary-to-secondary stream velocity also increased the mixing rate for shear layers of the same density ratio. In the present study, the secondary stream may be thought of as the ambient cold airflow induced by the entrainment of the HVOF jet. Quantitative comparisons of the present cases depicted in Fig. 6(b) and 7 would require temperature and velocity measurements, which have not been made in this preliminary study.

It is important here to make a strong distinction between density-ratio effects on turbulent mixing and compressibility effects per se. It has been shown (Ref 13) that compressibility tends to

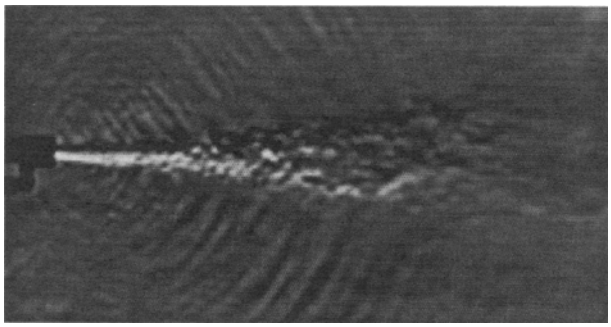

**Fig. 7** Microsecond schlieren image of a cold-gas mixing plume. Jet velocity ~ 500 m/s (1640 ft/s); $\rho_{jet}/\rho_{atm} \sim 2$

decrease the turbulent mixing of a high-speed mixing layer compared to that of a low-speed mixing layer *at the same ratio of densities*. Gas compressibility becomes important in this context when the difference in speed between two mixing streams (such as the HVOF jet and the atmosphere) is significant when compared to the speed of sound in either of the streams. However, the effects of density ratio and jet velocity clearly outweigh the influence of compressibility in the present case, as the hot jet has a spreading rate that is significantly greater than that of the cold jet.

The ratio of chamber pressure to atmospheric pressure in these experiments was varied from about 6 to 9 for both the hot- and cold-gas cases; no significant effect on mixing was observed. It is believed that this pressure variation within the operating range of the HVOF system is not sufficient to change the overall jet-to-atmosphere density ratio significantly. Furthermore, no measurable difference in mixing was detected for the two different barrel lengths tested; as mentioned earlier, the properties at the barrel exit plane do not appear to be strongly affected by barrel length.

As already noted, mixing of the high-speed HVOF jet with the oxidizing atmosphere is likely to be detrimental to coating quality, because sprayed particles at elevated temperatures are exposed to possible oxidation prior to formation of the coating. Ironically, a significant effort in SCRAMJET-propulsion research (Ref 13) since 1985 has been aimed at *increasing* compressible turbulent mixing rates. Knowledge gained in that effort may now be of help in *decreasing* the mixing of the HVOF spray with the atmosphere.

### 3.4 *Jet Noise*

Figure 8, a schlieren image of the HVOF jet with a microsecond exposure time, shows the emission of strong jet noise near the exit of the jet. The density fluctuations associated with the noise and made visible by the schlieren technique propagate into the atmosphere on either side of the HVOF jet. Such jet-noise emissions are not directly related to sprayed coating quality, but are nonetheless a nuisance factor in all thermal spraying. They arise from the interaction of the vortical structures of the turbulent mixing layer with the "shock diamonds," as illustrated in Fig. 9, where the focus of each shock cell becomes a radiator of acoustic energy. The intensity of this jet noise is proportional to the shock-wave strength in the shock cells, and the acoustic wavelength of peak noise emission is comparable to the length of a shock cell (Ref 14). As shown in Fig. 8, this noise radiation is highly directional in a conical region whose axis is the jet centerline and whose vertex is the barrel exit.

Although jet noise is not the focus of the present research, it is a secondary consequence of HVOF spraying that is hard to ignore. No obvious effects of either chamber pressure or barrel length on the noise were noted, although microphone measurements in an anechoic chamber would be required to make a definite statement in this regard. Supersonic jets in the open air will never be "whisper-quiet," but research performed on the jet noise of aerospace propulsion units has indicated some ways of alleviating this problem.

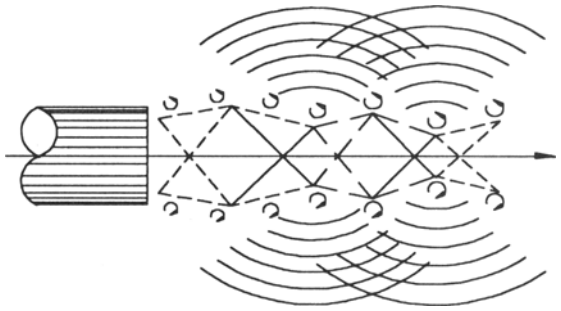

**Fig. 9** Diagram of jet-noise generation. Source: adapted from Ref 14

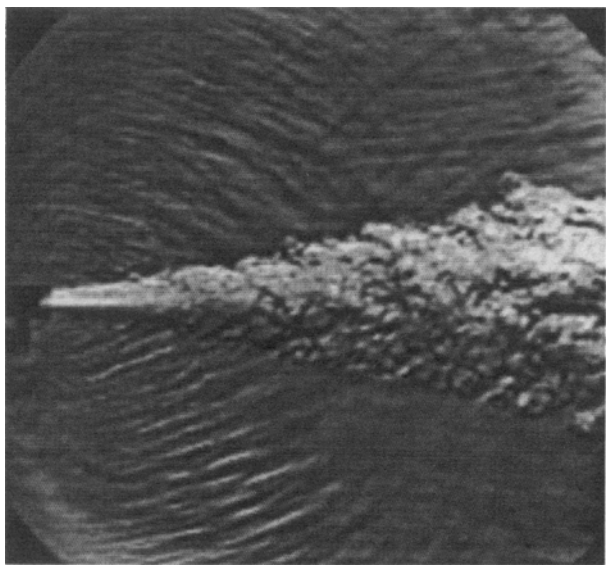

**Fig. 8** Microsecond schlieren image showing emission of jet-noise as circular wave patterns originating near the exit of the hot HVOF jet

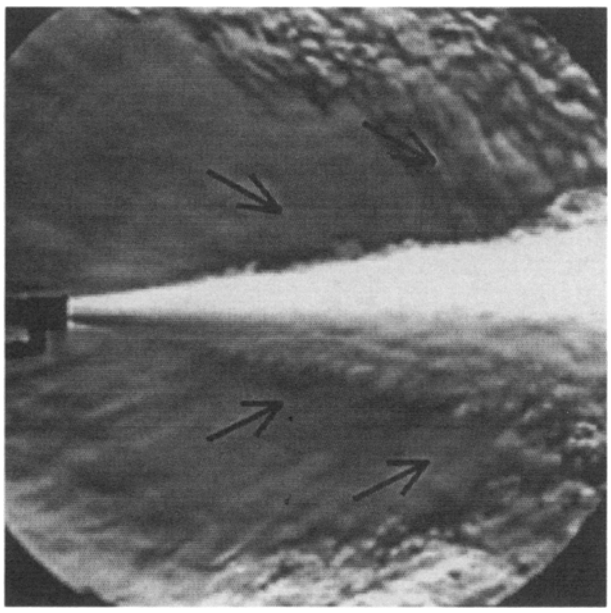

**Fig. 10** Full-field schlieren image showing in the entrainment of surrounding air into the mixing plume as indicated by arrows

### 3.5 *Entrainment*

The intense turbulent mixing of the HVOF jet entrains, or "gulps," the surrounding atmosphere. This effect is so strong that a bulk airflow is induced in the vicinity of the HVOF jet along the direction of its axis. In close quarters, large recirculation zones can be set up by this phenomenon. As indicated by the arrows in Fig. 10, the hot gas of the jet recirculates along the floor and ceiling of the laboratory and is once again drawn into the mixing plume. As in the example of a high-pressure ejector, a supersonic freejet can move many times its own mass flux by entrainment of the surrounding air.

Again, secondary airflow and the entrainment of unwanted particulate matter is not expected to be a primary issue in the quality of HVOF sprayed coatings. It could present a problem when spraying in a dirty environment, where contaminants drawn into the jet could become embedded in the coating. It also requires that some thought be given to the secondary airflow in spraying booths, especially in terms of recirculation and proper venting.

## 4. Conclusions

Optical flow-visualization techniques have been used to examine the gas-dynamic behavior of the hot supersonic jet produced by an HVOF thermal spray gun. The principles of gas dynamics impact the spray process in several ways. Of primary importance is the transfer of heat energy and momentum from the gas to the particles being sprayed as well as the rapid turbulent mixing of the jet with the ambient atmosphere. Visualizations of the HVOF flowfield reveal a broad mixing region surrounding the visible, high-temperature core of the jet. The supersonic core of the jet is dissipated by mixing, and the jet reaches subsonic velocities well before recommended spray standoff distances. Furthermore, since turbulent mixing transports atmospheric oxygen to the center of the jet, it is possible that oxidation of spray particles might occur during flight. Thus, it can be assumed that such mixing is potentially detrimental to coating quality. The significant factors influencing the mixing appear to be the velocity of the jet and the ratio of jet density to the density of the ambient atmosphere. The visualizations of the HVOF plume also reveal strong jet-noise radiation as well as the induced motion and recirculation of the surrounding atmosphere.


## Acknowledgments

The authors thank Lori J. Dodson and Dr. Jonathan W. Naughton of the Gas Dynamics Laboratory for their contributions to this effort. The research is sponsored by DOE Grant DE-FG02-92ER14302, monitored by Dr. Oscar Manley. The cooperation of Merle and Richard Thorpe of Hobart-Tafa Technologies, Inc., is gratefully acknowledged.


## References


1. K.A. Kowalsky, D.R. Marantz, M.F. Smith, and W.L. Oberkampf, HVOF: Particle, Flame Diagnostics and Coating Characteristics, *Thermal Spray Research and Applications*, T.F. Bernecki, Ed., ASM International, 1991, p 587-592
2. M.L. Thorpe and H.J. Richter, A Pragmatic Analysis and Comparison of the HVOF Process, *Thermal Spray: International Advances in Coating Technology*, C.C. Berndt, Ed., ASM International, 1992, p 137-147
3. E.B. Smith, G.D. Power, T.J. Barber, and L.M. Chiappetta, *Thermal Spray Coatings: Properties, Processes, and Applications*, T.F. Bernecki, Ed., ASM International, 1992, p 805-810
4. G.D. Power, T.J. Barber, and L.M. Chiappetta, "Analysis of a High Velocity Oxygen-Fuel (HVOF) Thermal Torch," Paper 92-3598, AIAA/SAE/ASME/ASEE 28th Joint Propulsion Conference and Exhibit (Washington, DC), AIAA, 1992
5. G.P. Sutton, *Rocket Propulsion Elements*, 6th ed., John Wiley & Sons, 1992
6. W. Merzkirch, *Flow Visualization*, Academic Press, 1987
7. G.S. Settles, Colour-Coding Schlieren Techniques for the Optical Study of Heat and Fluid Flow, *Int. J. Heat Fluid Flow*, Vol 6, 1985, p 3-15
8. M.A. Saad, *Compressible Fluid Flow*, Prentice-Hall, 1985, p 190-291
9. C.P. Donaldson and R.S. Snedecker, A Study of Free Jet Impingement, Part 1. Mean Properties of Free and Impinging Jets, *J. Fluid Mech.*, Vol 45 (Part 2), 1971, p 281-319
10. K.S. Abdol-Hamid and R.G. Wilmoth, Multiscale Turbulence Effects in Underexpanded Supersonic Jets, *AIAA J.*, Vol 27 (No. 3), 1989, p 315-322
11. O. Knotek and U. Schnaut, Numerical Simulation of the Influences of HVOF Spraying Parameters on Coating Properties, *Thermal Spray Coatings: Research, Design, and Applications*, C.C. Berndt and T.F. Bernecki, Ed., ASM International, 1993, p 7-12
12. G.L. Brown and A. Roshko, On Density Effects and Large Scale Structure in Turbulent Mixing Layers, *J. Fluid Mech.*, Vol 64 (Part 4), 1974, p 775-816
13. D. Papamoschou and A. Roshko, The Compressible Turbulent Shear Layer: An Experimental Study, *J. Fluid Mech.*, Vol 197, 1988, p 453-477
14. S.P. Pao and J.M. Seiner, Shock Associated Noise in Supersonic Jets, *AIAA J.*, Vol 21 (No. 5), 1983, p 687-693